基于四(3-吡啶氧亚甲基)甲烷及氰化铜螺旋链手性
金属有机骨架化合物的合成及其性质研究

江 靖[1]　任世斌*,[1,2]　林勇强[1]　吴 涛[2]　张小鹏[2]

韩得满[1]　梁华定[1]　李 芳[1]　贾文平*,[1]

([1] 台州学院医药化工学院,台州　317000)
([2] 南京大学化学化工学院配位化学国家重点实验室,南京　210093)

摘要：通过一个非手性配体和 1D 氰化铜链螺旋成功构建了一种新型的手性金属有机骨架：$[Cu_4(CN)_4(L)_2]_n$ (**1**,L=四(3-吡啶氧亚甲基甲烷))；铜(I)和原位生成的氰基组装而生成的螺旋是左旋并且它使得金属有机框架具有手性。这是首例通过半刚性四面体配体多变的构像诱导合成独特的手性金属有机骨架化合物。此外还研究了该化合物的手性、热稳定性以及介电性质。

关键词：手性金属有机骨架；半刚性四面体配体；螺旋 CuCN 链；介电性质

Synthesis of Chiral Metal-Organic Framework and Study of Its Properties
Based on Tetrakis(3-pyridyloxymethylene)methane and Helical CuCN Chains

JIANG Jing[1]　　REN Shi-Bin*,[1,2]　　LIN Yong-Qiang[1]　　WU Tao[2]

ZHANG Xiao-Peng[2]　　HAN De-Man[1]　　LIANG Hua-Ding[1]　　LI Fang[1]　　JIA Wen-Ping*,[1]

([1] *School of Pharmaceutical and Chemical Engineering, Taizhou University, Taizhou, Zhejiang* 17000, *China*)
([2] *State Key Laboratory of Coordination Chemistry, School of Chemistry and*
Chemical Engineering, Nanjing University, Nanjing 210093, *China*)

Abstract: A novel homochiral metal-organic framework is successfully constructed by an achiral ligand and 1D helical CuCN chains: $[Cu_4(CN)_4(L)_2]_n$ (L=tetrakis(3-pyridyloxymethylene)methane) (**1**); the helixes assembled by copper(I) and CN groups in situ generated are left-handed and transform the framework to chiral. This is the first example of chiral MOFs induced by flexible conformation of semigrid tetrahedral ligand. In addition, the chiral property of bulk products is confirmed by VCD spectra, the thermal stability and dielectric properties are also investigated. CCDC: 921046.

Key words: chiral metal-organic framework; semigrid tetrahedral ligand; helical CuCN chains; dielectric properties

　　Homochirality and helicity often coexist in the living world. Many natural chiral complexes, like Protein, Enzymes, nucleic acids and other biopolymers are in the possession of a definite helicity[1-2]. Therefore, the study of the relationship between chirality and helicity within the same complex is of importance to

understand generation of chiral materials.

Homochiral porous MOFs are widely used in many practical applications, such as asymmetric catalysis [3], enantioselective separations [4], nonlinear optical materials [5]. The key to the construction of homochiral MOF materials is the careful selection of chiral ligands, achiral building blocks or chiral molecules or charge-balanced ions, which play an important role in the self-assembly of homochiral MOF[6]. In addition, synthetic modification of the organic struts or the metal nodes are readily applicable to the construction of a homochiral MOF [7]. To date, the synthesis of chiral MOFs from achiral ligands is a key issue in studying the genesis of chirality. However, the genesis mechanism of chirality remains one of the most challenging tasks. To the best of our knowledge, homochiral MOFs are not reported with mutually perpendicular helices.

To investigate the generation of homochiral materials with achiral ligands, we have introduced a kind of tetrahedral ligand as the tectons in our study. Due to its specific configuration, it can be used to prepare a series of new coordination polymers with intriguing structures [8]. However, homochiral MOFs based on tetrahedral ligands remain largely unexplored so far. Herein, we obtain another novel homochiral MOF [Cu$_4$(CN)$_4$(L)$_2$]$_n$ (**1**) with another tetrahedral ligand tetrakis (3-pyridyloxymethylene) methane (L). It is character-ized by X-ray crystallography, elemental analysis, infr ared spectra (IR), powder X-ray diffraction (PXRD) and thermogravimetric (TG) analyses. In addition, their dielectric properties have also been discussed.

1 Experimental

1.1 Materials and physical measurements

L was prepared according to the literature method[9]. All other chemicals were from commercial source without further purification. Elemental analyses of C, H, N were determined with a Perkin-Elmer 2400C elemental analyzer. Infrared spectra were recorded in the range of 400~4 000 cm^{-1} on a Vector 22 Bruker spectrophotometer with pressed KBr pellets. Thermal analysis (TG) was carried out in a nitrogen stream using Seiko Extar 6000 TG/DTA equipment with a heating rate of 10 ℃·min^{-1}. X-ray powder diffraction (XRD) patterns were measured using a Rigaku D/max-RA diffractometer with Cu $K\alpha$ radiation. Dielectric properties were also carried out using a Keithley 3330 Model LCZ meter to measure the dielectric constant as well as the dielectric loss.

1.2 Preparation of 1

The synthesis of **1**: orange single crystals of **1** were grown from solvothermal reaction of Cu(NO$_3$)· 6H$_2$O (0.096 6 g, 0.20 mmol), L (0.044 6 g, 0.1 mmol) and 2,4,6-tricarboxylpyridine (0.021 3 g, 0.1 mmol) in a mixed solvent of CH$_3$CN and H$_2$O (3:3, V:V) in a 30 mL acid-digestion bomb at 140 ℃ for 3 d. The product was washed with ethanol and dried in air. **1** was isolated as a single-phase product (yield:42.5% based on L). Anal. C$_{27}$H$_{24}$Cu$_2$N$_6$O$_4$, Calcd.(%): C, 52.00; H, 3.88; N, 13.48. Found (%): C, 51.81; H, 3.85; N, 13.46. IR (KBr, cm^{-1}): 2 102.41 s, 1 573.91s, 1 469.76s, 1 427.32s, 1 404.18w, 1 271.09s, 1 238.30s, 1 186.22m, 1 116.78m, 1 103.28w, 1 051.20s, 1 028.06s, 1 014.56s, 979.84s, 931.62m, 908.47w, 802.39 w, 700.16 w.

1.3 Crystallographic measurements

The single-crystal X-ray data collection for **1** were performed on a Bruker SMART APEX CCD diffractometer with graphite-monochromated Mo $K\alpha$ radiation (λ=0.071 073 nm) at room temperature. Data reductions and absorption corrections were performed using the SAINT and SADABS software packages, respectively. The structure was solved by direct methods and refined by full matrix least-squares methods on F^2 using the SHELXS-97 and SHELXL-97 programs[10]. Anisotropic displacement parameters were refined for all non-hydrogen atoms. The hydrogen atoms of the coordination water molecules and ligands were included in the structure factor calculation at idealized positions by using a riding model and refined isotropically. Metal atoms in each complex were located from the E-maps and All non-hydrogen atoms were refined anisotropically. The relevant crystallogra-phic data are presented in Table 1 and selected bond lengths and angles are given in Table 2.

CCDC: 921046.

Table 1　Crystal data and structure refinement for complex 1

Complex	**1**	V / nm³	2.604.2(5)
Chemical formula	$C_{27}H_{24}Cu_2N_6O_4$	T / K	296(2)
Formula weight	623.6	Z	4
Flack	0.02(3)	D_c / (g·cm⁻³)	1.591
Space group	$P4_32_12$	R_1 $(I>2\sigma(I))$	0.043 6
a / nm	0.894 93(9)	wR_2 $(I>2\sigma(I))$	0.111 1
b / nm	0.894 93(9)	R_1 (all data)	0.047 5
c / nm	0.325 16(5)	wR_2 (all data)	0.113 8

$R_1=\sum||F_o|-|F_c||/\sum|F_o|$, $wR=[\sum w(F_o^2-F_c^2)^2/\sum w(F_o^2)^2]^{1/2}$.

Table 2　Selected bond distances (nm) and angles (°) for complex 1

C14-Cu1	0.190 4(4)	Cu1-N2	0.215 5(3)	N3-Cu1ⁱⁱ	0.198 2(4)
Cu1-N3ⁱ	0.198 2(4)	Cu1-N1	0.216 5(3)		
C14-Cu1-N2	10.776(16)	C14-Cu1-N1	11.564(16)	N2-Cu1-N1	10.290(13)

Symmetry transformations used to generate equivalent atoms: ⁱ $0.5+x$, $1.5−y$, $0.25−z$; ⁱⁱ $−0.5+x$, $1.5−y$, $0.25−z$.

2　Results and discussion

2.1　Synthesis of complex 1

1 was synthesized by the solvothermal reaction of $Cu(NO_3)_2$, L and 2,4,6-tricarboxylpyridine in the mixed-solvent system of CH_3CN and H_2O. Attempts to prepare other complexes using cadmium nitrate, zinc nitrate, cobalt nitrate instead of copper nitrate under similar conditions have so far met with failures. In addition, no corresponding complexes are formed by changing solvent component. The preparation of **1** in the presence of acetonitrile were very successful, probably because the CN groups in **1** were in situ generated from the cleavage of acetonitrile molecules via copper catalysis. Single crystal X-ray diffraction have showed that **1** consists of CN groups. In addition, The FT-IR spectrum of **1** also confirm the presence of the CN group by a strong peak at 2 123 cm⁻¹.

2.2　Descriptions of crystal structures

Complex **1** crystallizes in the tetragonal chiral space group $P4_32_12$ and its asymmetric unit contains one crystallographically independent Cu atoms, one cyanide groups and one half of L ligand. As shown in Fig.1, each of Cu atom has tetrahedral geometry, coordinated by two cyanides and two nitrogen atoms from L. The Cu-X (X=C, N) bonds are in range of 0.190 4(4)~0.216 5(3) nm, and X-Cu-X angles are between 97.42 (15)°~126.85 (17)°. The bond valence sum calculations for Cu (0.91) suggest that Cu is monovalent, which confirm that Cu atom adopt the tetrahedral geometry. The L ligand with the quaternary carbon atom sitting on the S4 tetrahedron center is in a distorted tetrahedral coordination geometry with the angles between four arms ranging from 108.13° to 111.07°. Each L coordinates four neighboring Cu ions through its four peripheral pyridyl groups. In addition, as a bridging ligand each cyanide group is coordinated to two adjacent Cu centers and the resulting helical Cu-CN chains are formed with the Cu⋯Cu distances of 0.498 5(1) nm (Fig.2).

As shown in Fig.3, a interesting feature in **1** is that helical CuCN chains are mutually perpendicular
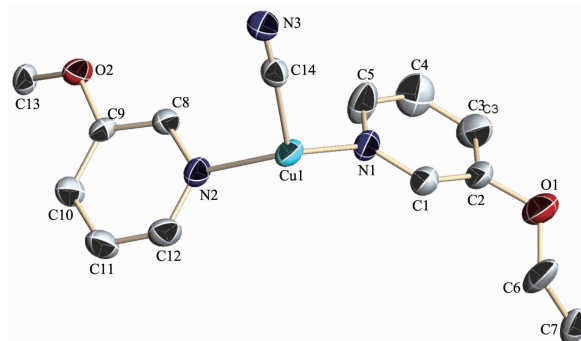
H atoms are omitted for clarity

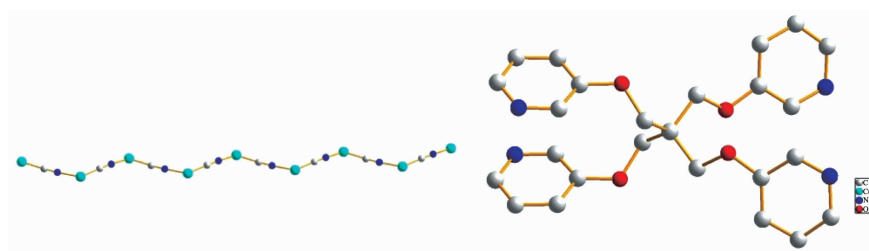Fig.1　An ORTEP drawing of the asymmetric unit of complex **1** at the 50% probability

Fig.2　View of the organic ligand and CuCN helical chain used in this paper
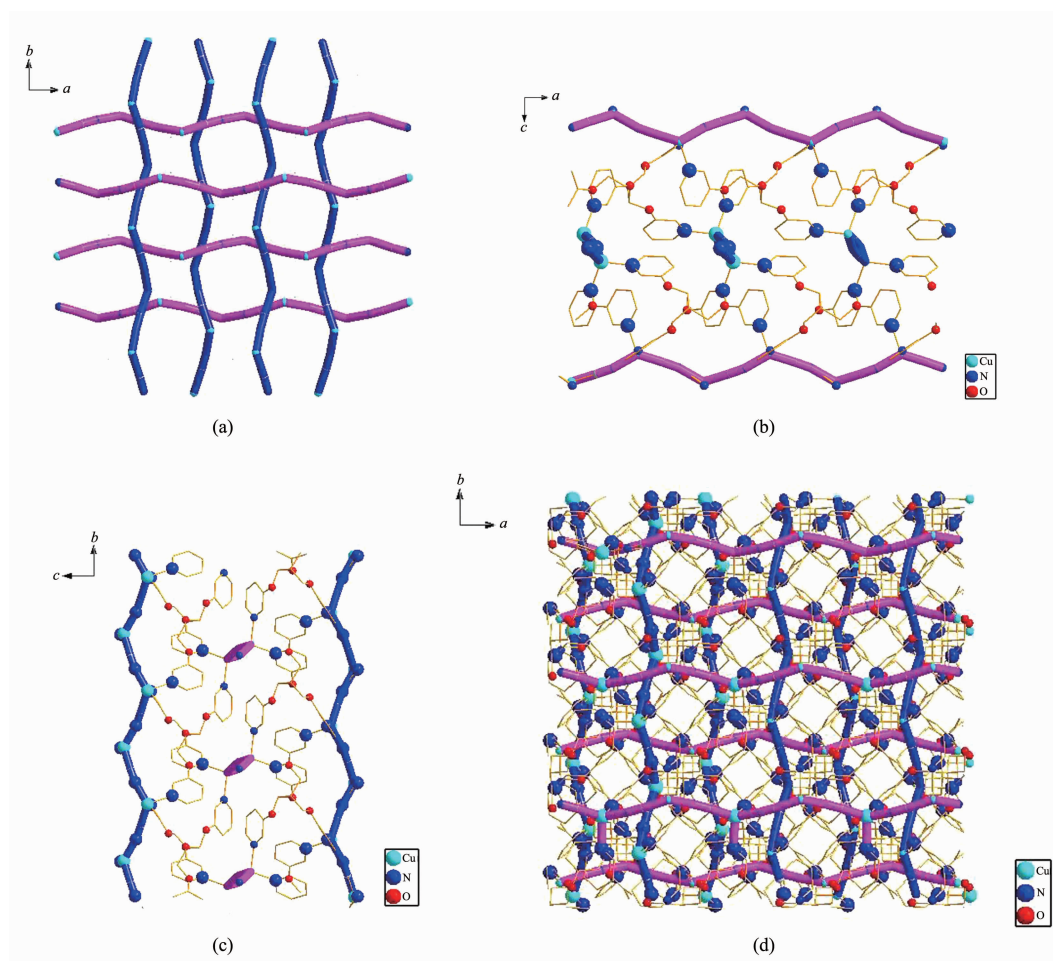

Fig.3　View of mutually perpendicular CuCN helices (a); The 3D framework of **1**, which is composed of
CuCN helices along the *b*, *a* and *c* axis (b, c, d)

(Fig.3a). The helical CuCN chains are aligned in parallel along the *a* and *b* axle, respectively, which are linked together by the bridge of L to form a 3D framework (Fig.3b~d). Another feature in **1** is non-interpenetrated. Due to various N-donor orientations of L, helical CuCN chains can coordinates via Cu atom with N atoms to form 3D framework. By varying N-atom position of the bridging ligands, the total solvent-accessible volumes are correspondingly decreased from 6.3% to almost zero by PLATON

calculations[11]. The complex **1** exhibits hardly any adsorption for N_2 and H_2 at 77 K under low pressure, which confirm that no pores and channels in **1** can accommodate N_2 and H_2 gas molecules. This can be ascribe to the existence of mutually perpendicular helices, which can block the pores and channels in **1**. Thus, the observations on their structures seem to show that alteration of isomeric ligands bring on a significant difference in the structure diversity based on these coordination polymers.

2.3　XRD and thermal stability

To confirm whether the crystal structures are truly representative of the bulk materials, PXRD experiments were carried out for **1**. The peak positions of the experimental and simulated XRPD patterns are in agreement with each other, which show that the synthesized bulk materials and the measured single crystals are the same　(Fig.4). Thermogravimetric (TG) analysis for **1** was studied to reveal their thermalstability. As seen in Fig.5, a little weight loss from room temperature to 251.2 ℃ is attributed to surface water molecules and the decomposition temperature of the residual composition spans the range of 251.2~421.9 ℃. This result may indicate that complex **1** is highly thermal stable.
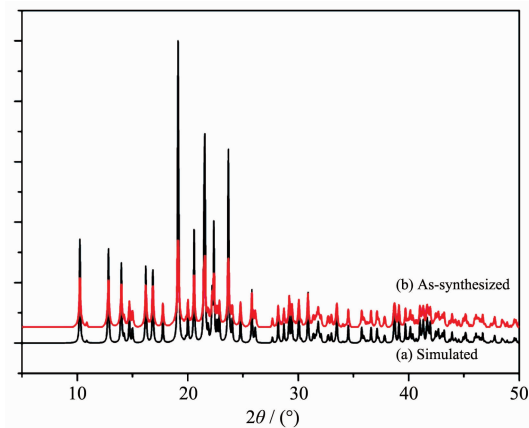

Fig.4　PXRD Pattern of **1** in the solid state

2.4　VCD and IR spectroscopy

The IR spectra of **1** exhibits strong characteristic absorptions of the py groups for C-C skeleton vibration at 1 428, 1 468, 1 577 cm^{-1} and the C-H bending virbration at 696, 808 cm^{-1}. The strong
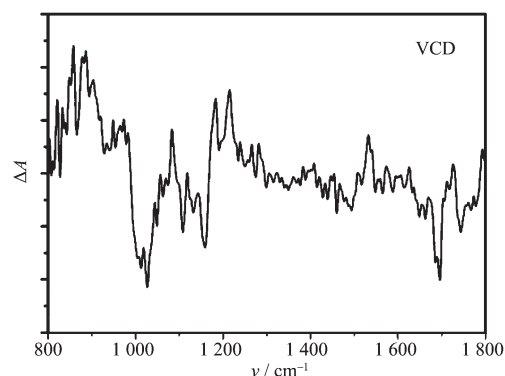

Fig.5　Solid-state VCD of **1**

absorptions centered at 2 012 cm^{-1} is a characteristic of C≡N group stretching vibration.

VCD spectroscopy is a very powerful technique to obtain conformational information of chiral complexes. The VCD spectra of **1**, which were measured using a few crystals of **1**, show strong signals corresponding to the absorptions of their IR spectra, indicating the crystals of **1** are chiral (Fig.5). In addition, bulk crystals of **1** were crushed to powder and mixed adequately. The sample also displays strong VCD signals. On the basis of the above experimental results, it may be infered that the crystallization of **1** are enantiomeric excess rather than racemic.

2.5　Dielectric properties

Dielectric measurements were performed on a pellet specimen of **1** coated with Ag-glue, between a frequency 0.96 Hz to 10 MHz. Fig.6 shows the variation of dielectric constant with the frequency of the external field at the room temperature. At the lower frequencies, the dielectric constant is found to
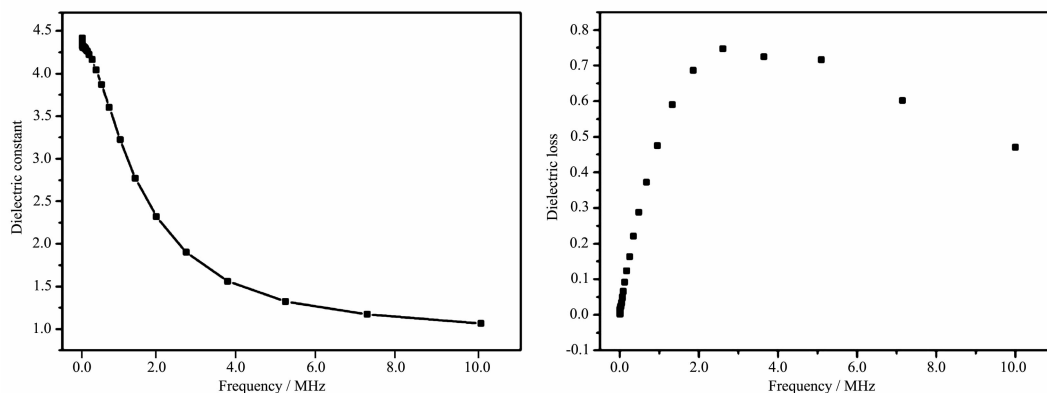

Fig.6　(a) Dielectric constant (ε_r) and (b) dielectric loss vs frequency for **1**

be considerably higher than that at higher frequencies, which can be attributed to the interfacial polarization, in which the mobile charge carriers are impeded by a physical barrier that inhibits producing a localized polarization of the material[11]. At a higher frequencies, the dielectric constant of the complex becomes almost constant and it is found to be 1.06 for 7.14 MHz at 298 K. In addition, the dielectric loss of **1** at lower frequencies assume low values. The dielectric loss was found to reach a maximum value 0.75 for a frequency of 2.6 MHz. The study on these materials will maybe provide some valuable information for exploiting novel dielectric materials.

3 Conclusions

In summary, the complex reported here is an unprecedented example of a homochiral MOF, which consists of mutually perpendicular helical CuCN chains and an achiral ligand. The synthetic method employed in this study may provide a new means of constructing a homochiral MOF without any chiral ligand. These materials are of great interest because of their potential applications in nonlinear optical materials, asymmetric catalysis and separation, ferroelectrics and chiral magnets.

Reference:

[1] (a)Mason S F. *Molecular Optical Activity and the Chiral Discriminations*. Cambridge: Cambridge University Press, **1982**.
(b)Bonner W A. *Origins Life Evol. Biosphere*, **1994**:63

[2] Loewenstein W R. *Touchstone of Life Molecular Information*: *Cell, Communication, and the Foundations of Life*. Oxford: Oxford University Press, **1999**.

[3] (a)Gruselle M, Train C, Boubekeur K, et al. *Coord. Chem. Rev.*, **2006,250**:2491-2500
(b)Chelucci G, Thummel R P. *Chem. Rev.*, **2002,102**:3129-3170

[4] (a)Zhang J, Chen S M, Wu T, et al. *J. Am. Chem. Soc.*, **2008, 130**:12882-12883
(b)Bu X H, Tong M L, Chang H C, et al. *Angew. Chem., Int. Ed.*, **2004,43**:192-195

[5] (a)Wen H R, Wang C F, Song Y, et al. *Inorg. Chem.*, **2005, 44**:9039-9045
(b)Meng X R, Song Y L, Hou H W, et al. *Inorg. Chem.*, **2003,42**:1306-1315

[6] (a)An H Y, Wang E B, Xiao D R, et al. *Angew. Chem. Int. Ed.*, **2006,45**:904-908
(b)Zhu Q, Sheng T, Fu R, et al. *Chem. Commun.*, **2010,46**: 9001-9003
(c)Liang X Q, Jia J T, Wu T, et al. *CrystEngComm*, **2010,12**: 3499-3501
(d)Lin Z, Slawin A M Z, Morris R E. *J. Am. Chem. Soc.*, **2007,129**:4880-4881

[7] Banerjee M, Das S, Yoon M, et al. *J. Am. Chem. Soc.*, **2009, 131**:7524-7525

[8] (a)Ren S B, Zhou L, Zhang J, et al. *CrystEngComm*, **2009, 11**:1834-1836
(b)Ren S B, Zhou L, Zhang J, et al. *Inorg. Chem. Commun.*, **2011,14**:558-561

[9] Zhang Q, Bu X, Lin Z, et al. *Inorg. Chem.*, **2008,47**:9724-9726

[10](a)Sheldrick G M. *SHELXS*-97, *Programs for X-ray Crystal Structure Solution*, University of Göttingen, Göttingen, Germany, **1997**.
(b)Sheldrick G M. *SHELXL*-97, *Programs for X-ray Crystal Structure Refinement*, University of Göttingen, Göttingen, Germany, **1997**.

[11]Spek A L. *PLATON*, *A Multipurpose Crystallographic Tool*, Utrecht University, Utrecht, **1999**.

[12]Kumar G R, Raj S G, Mohan R, et al. *Cryst. Growth Des.*, **2006,6**:1308-1310